

ANALYSIS OF FUNDAMENTAL AND SYSTEMATIC EFFECTS LIMITING HYDROGEN MASER FREQUENCY STABILITY

Edward M. Mattison
Robert F.C. Vessot

Smithsonian Astrophysical Observatory
Cambridge, Massachusetts 02138

INTRODUCTION

The hydrogen maser is currently one of the most stable frequency standards currently available, providing frequency stabilities of several parts in 10^{16} for averaging times of $10^3 - 10^4$ seconds. Further improvement to the stability of hydrogen masers requires a comprehensive understanding of the relative magnitudes of physical processes that influence frequency stability. We discuss an approach to understanding a variety of thermodynamic and systematic processes that can affect maser frequency stability.^[1] This examination enables the maser researcher and user to identify stability-limiting effects and thus to choose areas where improvements could lead to increased stability. As is true with many complex systems, overall improvements can generally be gained only by attending simultaneously to a variety of factors. Improving one aspect of the maser will not significantly increase the frequency stability if variations in another area limits the stability to a level comparable to the first.

The hydrogen maser's frequency stability is affected by fundamental thermal noise and by systematic effects. The maser frequency stability, expressed by the two-sample, or Allan, deviation^[2] $\sigma(\tau)$ typically has three approximately linear portions when displayed on a log-log plot.

For values of the averaging interval τ between approximately 1 and 100 seconds, $\sigma(\tau)$ is approximately proportional to τ^{-1} . This behavior results from thermally-induced phase noise within the bandwidth of the maser's receiver system. Between roughly 100 and 1000 seconds $\sigma(\tau)$ is proportional to $\tau^{-1/2}$; in this range of averaging interval, the frequency stability is determined by thermal noise within the hydrogen atomic linewidth. For longer averaging times $\sigma(\tau)$ is generally found to vary with τ between $\tau^{1/2}$ and τ^1 . τ^1 behavior is characteristic of linear frequency drift, while $\tau^{1/2}$ behavior is termed random walk of frequency.

FUNDAMENTAL STABILITY EFFECTS DUE to THERMAL NOISE

The Allen deviation $\sigma_L(\tau)$ due to thermal noise within the atomic linewidth is given by^[3]

$$\sigma_\ell(\tau) = \frac{1}{Q_\ell} \sqrt{\frac{kT}{2P\tau}} \quad (1)$$

Here Q_ℓ is the atomic line Q, k is Boltzmann's constant, T is the absolute temperature within the maser's resonant cavity, and P is the power delivered by the atomic beam to the cavity.

The effect of thermal noise on the maser's receiver is given by^[4]

$$\sigma_r(\tau) = \frac{1}{\omega\tau} \sqrt{\frac{FkTB}{P_r}} = \frac{1}{\omega\tau} \sqrt{\frac{FkTB}{P} \left(\frac{1+\beta}{\beta} \right)} \quad (2)$$

Here F is the noise figure of the receiver system, B is the receiver's effective noise bandwidth, P_r is the power delivered by the maser cavity to the receiver, β is the cavity coupling factor, and $\omega = 2\pi f_m$, where f_m is the maser transition frequency, 1420.405...MHz.

It is necessary to express the frequency stability in terms of quantities that are either measurable or controllable, such as the coupling factor, cavity Q, and hydrogen flux. These parameters enter the Allan variance through the line Q and the beam power.

The power radiated by the beam can be expressed^[3] in terms of the net flux I of radiating atoms entering the storage volume, that is, the difference between the number of atoms entering in the hyperfine state "c" ($F=1, m_F=0$) and the number in the state "a" ($F=0, m_F=0$).

$$P = \frac{\hbar\omega}{2} I_{th} \left[-2q^2 \left(\frac{I}{I_{th}} \right)^2 + (1 - cq) \left(\frac{I}{I_{th}} \right) - 1 \right] \quad (3)$$

where I_{th} , the minimum flux required for oscillation in the absence of spin exchange, is given by

$$I_{th} = \frac{\hbar V_c}{4\pi\mu_o^2 Q_c \eta} \gamma_t^2 \quad (4)$$

and the parameter q is defined by

$$q = \frac{\sigma \bar{v}_r \hbar}{8\pi\mu_o^2} \frac{\gamma_t}{\gamma_d} \frac{V_c}{\eta V_b} \frac{1}{Q_c} \frac{I_{tot}}{I} \quad (5)$$

Here μ_o is the Bohr magneton, σ is the spin-exchange cross section, \bar{v}_r is the relative hydrogen velocity in the storage bulb, V_c is the resonant cavity volume, η is the storage bulb's filling factor and Q_c is the loaded cavity Q. In most masers (I_{tot}/I) ≈ 2 because the state selection magnet focusses atoms in both states "c" and "d" ($F=1, m_F=1$) into the storage bulb. If single state selection is used, only state "c" atoms enter the bulb and (I_{tot}/I) ≈ 1 . γ_t is the total density-independent relaxation rate and γ_d is the rate at which atoms are removed from the storage bulb by escape through its entrance collimator and by recombination on the wall surface. Generally, γ_t exceeds γ_d because to magnetic inhomogeneity relaxation and to wall relaxation processes other than recombination; in a properly built maser (γ_t/γ_d) ≈ 1 . Under similar assumptions, the parameter c in Eq. 3 has the value $c = 3$.

The atomic line Q is also related to the flux and the relaxation rates:

$$Q_\ell = \frac{\omega}{2\gamma_2} = \frac{\omega}{2\gamma_t} \left[1 + q \left(\frac{I}{I_{th}} \right) \right]^{-1} \quad (6)$$

To find the level of flux that minimizes the Allan variance $\sigma^2(\tau)$, we can express $\sigma^2(\tau)$ as a function of flux by substituting Eqs. (3) and (6) into Eqs. (1) and (2) and finding the minimizing flux by differentiating with respect to I . It is physically reasonable that values of I exist that minimize $\sigma_\ell^2(\tau)$ and $\sigma_r^2(\tau)$. $\sigma_r^2(\tau)$ is proportional to P^{-1} ; since P is a quadratic function of I with a maximum (resulting from spin exchange relaxation overwhelming the increase in power with increasing flux), $\sigma_r^2(\tau)$ has a corresponding minimum. $\sigma_\ell^2(\tau)$ is proportional to $[Q_\ell^2 P]^{-1}$. At low flux levels, Q_ℓ has a maximum value determined primarily by atomic loss mechanisms described by γ_d , and its value decreases with increasing flux. Thus the product $Q_\ell^2 P$ has a maximum at a smaller value of flux than does P alone, and $\sigma_\ell^2(\tau)$ has a corresponding minimum at a smaller value of flux than does $\sigma_r^2(\tau)$.

Minimization of $\sigma_\ell(\tau)$

We wish to find maser operating conditions that minimize the Allan variance $\sigma_\ell^2(\tau)$, and thus the Allan deviation $\sigma_\ell(\tau)$. For a given maser the readily variable parameters are the flux I , cavity coupling factor β , and state selection ratio I_{tot}/I . We assume that Q_o , the maser's unloaded cavity Q , is fixed, since it is determined by the dimensions and materials of the maser's resonant cavity and storage bulb. (Altering the dimensions to change the bulb filling factor, however, can affect Q_o .) Then Q_c , the loaded cavity Q , is determined by the coupling factor:

$$Q_c = \frac{Q_o}{1 + \beta} \quad (7)$$

The parameter q can be expressed as

$$q = q_o(1 + \beta) \quad (8)$$

where q_o is independent of β and is defined by

$$q_o = \frac{\sigma \bar{v}_r \hbar}{8\pi\mu_o^2} \frac{\gamma_t}{\gamma_d} \frac{V_c}{\eta V_b} \frac{1}{Q_o} \frac{I_{tot}}{I} \quad (9)$$

It is convenient to introduce the normalized flux variable

$$x = q \frac{I}{I_{th}} \equiv \frac{\gamma_{2se}}{\gamma_t} \quad (10)$$

By expressing the beam power and line Q in terms of x and β and differentiating with respect to x , one can find^[1,5,6] the condition on flux that minimizes σ_ℓ^2 :

$$\tilde{x}_\ell = \frac{1 - q}{1 + q} \quad (11)$$

From Eq. 12 we can express Eq. 11 as

$$\left(\tilde{\gamma}_{2se} \right)_\ell = \gamma_t \left(\frac{1 - q}{1 + q} \right) \quad (13)$$

This means that for a particular value of cavity coupling, the minimum Allan variance due to thermal noise within the atomic linewidth occurs when the flux is adjusted so that the spin exchange relaxation rate γ_{2sc} equals the density independent relaxation rate γ_t decreased by the factor $(1 - q)/(1 + q)$. For many masers, particularly those employing single state selection, $q \ll 1$, and $(\tilde{\gamma}_{2sc})_t \approx \gamma_t$.

Minimization of $\sigma_r(\tau)$

The contribution to the Allan variance due to thermal noise at the maser receiver is given by Eq. 1. σ_r^2 is affected by the properties of the maser's receiver system through the noise figure F and noise bandwidth B , and by the maser's operating conditions through the beam power P and rf coupling factor β . One approach to reducing σ_r^2 is by reducing the noise figure and bandwidth. In practice this generally means narrowing the receiver's lock-loop bandwidth and employing a low-noise preamplifier. σ_r^2 can also be reduced by adjusting the maser's beam flux and the cavity's coupling constant β . The conditions for minimum value are established straightforwardly by setting the partial derivatives of Eq. 1 with respect to x and β equal to zero. The optimum value of flux is

$$\tilde{x}_r = \frac{1 - 3q}{4q} \quad (14)$$

For $q = 0.08$, a typical value using a traditional state selector, Eq. 14 gives $\tilde{x}_r = 2.38$, a level of flux that is difficult to achieve in practice due to limitations imposed by beam optics and scattering.

The optimizing value of β , for a value of $q_0 \sim 0.08$, is $\beta \simeq 14$. Such a large value of β would reduce the loaded cavity Q below the value required for oscillation, so that the optimizing value of β is unattainable. Then, to reduce σ_r^2 as much as possible, β should be made as large as possible consistent with the requirement for maser oscillation.

Characterization of Systematic Portion of Allan Variance

The expressions above for the Allan variance and the maser's operating conditions allow one to calculate the consequences of adjusting the various operating parameters. The mechanisms σ_r^2 and σ_t^2 contribute to the Allan variance for short ($< 10^2$ sec) and intermediate ($\sim 10^2$ to 10^5 sec) averaging times. To include the contributions of systematic effects, which dominate the stability for longer averaging times, one must model the long-term Allan variance. $\tau^{1/2}$ behavior, which has often been observed, is characteristic of random walk of frequency. As is shown in the later discussion of systematic processes, cavity pulling is a substantial source of systematic maser frequency variation. Maser frequency variations due to cavity pulling are proportional to the ratio (Q_c/Q_t) . Consequently we model the random walk component of σ by

$$\sigma_{RW}^2 = \xi \left(\frac{Q_c}{Q_t} \right)^2 \tau \quad (15)$$

Long-term measurements of a pair of VLG-11 masers give the value $\xi \left(\frac{Q_c}{Q_\ell} \right)^2 \sim 9 \times 10^{-36} \text{ sec}^{-1}$ for masers with $Q_c \sim 39 \times 10^3$ and $Q_\ell \sim 2 \times 10^9$; thus a reasonable value of ξ for comparison purposes is

$$\xi \sim 2.4 \times 10^{-26} \text{ sec}^{-1} \quad (16)$$

We shall assume that for masers with other values of Q_c and Q_ℓ , σ_{RW}^2 scales according to Eq. 15, with the value of ξ given by Eq. 16. Improved control of systematic frequency-pulling processes would be reflected in lower values of ξ .

Effect of Maser Operating Parameters on $\sigma(\tau)$

Using the expressions derived for the maser's operation we have calculated the Allan deviation $\sigma(\tau) = [\sigma_r^2(\tau) + \sigma_\ell^2(\tau) + \sigma_{RW}^2(\tau)]^{1/2}$ for a variety of operating parameters. The resulting graphs illustrate the benefits and tradeoffs that result from different choices of operating conditions.

To examine the effect of state selection, we consider a maser equipped with an adiabatic fast passage (AFP) state selection system. When the AFP system is off, $I_{tot}/I = 2$, and when the AFP system is on, the $F=1$, $m_F=1$ atoms are eliminated and $I_{tot}/I = 1$. Because q is proportional to I_{tot}/I , the AFP system reduces the value of q by half. Fig. 1 shows the calculated Allan deviation with the AFP system on and off. The values assumed for q_0 are typical of those measured in VLG-12 masers. For both curves we assume the flux is adjusted to give $x = 1$, approximately the value that minimizes $\sigma_\ell(\tau)$. (This assumption means that the total flux I_{tot} with AFP on would have to be twice as large as when AFP is off, in order to maintain the spin exchange relaxation rate γ_{se} equal to γ_t .) The curves show that, if the assumption $x = 1$ is satisfied, use of the AFP system would increase the frequency stability by a factor of approximately 2 for averaging intervals from 1 to about 10^3 seconds. The long-term stability is unaffected because γ_{sc} , and therefore the line Q, is constant under the assumption of constant x .

The effect of varying the beam flux, as measured by the parameter x , is shown in Fig. 2. Reducing x from 1 to 0.5 increases σ_ℓ only slightly, because Q_ℓ increases at the same time that P decreases. The deviation σ_r increases by about 30% due to the decrease in P , while σ_{RW} decreases by about 20% because Q_ℓ increases. Reducing the flux substantially, to $x = 0.15$, increases σ_r by a factor of about 3, and σ_ℓ by about twice, from their value for $x = 1$. These increases are due to the decrease in beam power and to the fact that the line Q decrease with flux is limited by the fixed value of γ_t . σ_{RW} is about 40% lower for $x = 0.15$ than for $x = 1$. We can see that a reduction of flux to the level of $x \sim 0.5$ would likely increase the long-term stability without substantially degrading the intermediate term stability from its optimum value.

Increasing the cavity coupling factor β decreases the loaded cavity Q and increases the rf power to the receiver. The decrease in Q_c reduces the cavity pulling effect, thereby improving the maser's long-term frequency stability, while the increase in receiver power

improves the stability for short averaging times. Increasing β also increases q , which decreases the beam power P , degrading the intermediate-term stability slightly. However, β cannot be increased indefinitely. In order for the maser to oscillate, the flux must be in a range set by the condition $P > 0$, which results in the limiting condition on q , $q < 0.172$. Using $q = q_0(1 + \beta)$ and $q_0 \sim 0.08$, typical for non-AFP operation, the limit on β is $\beta < 1.15$. For $\beta < 1.0$, the allowable range of flux reaches values accessible to both AFP and non-AFP operation. The effect of β on maser frequency stability is shown in Fig. 3 for $q_0 = 0.04$ (AFP on) and $x = 1$. Using a large coupling factor, $\beta = 1$, instead of a smaller value, $\beta \simeq 0.2$, improves the short-term stability at $\tau=1$ second by about 9%, degrades the intermediate term stability by about 15%, and improves the long-term stability by almost 40%, under the assumptions of our model.

The maser's long-term stability is determined by systematic processes. The stability can be improved by decreasing the sensitivity of maser components to external influences and improving their inherent long-term stability. Figure 4 shows the frequency stability improvement to be gained by decreasing the systematic effects by a factor of 2, assuming our model of a random walk of frequency proportional to the ratio Q_c/Q_ℓ . We discuss below a variety of systematic processes that can affect maser frequency stability.

SYSTEMATIC EFFECTS on HYDROGEN MASER FREQUENCY STABILITY

A great many physical effects can result in systematic maser frequency variations. It is impossible in the space available to present an analysis of more than a few; rather, it is our intention to describe a systematic approach to such an analysis, and to summarize the results of a more extensive study. A detailed analysis of identified effects is given in reference 1.

To analyze systematic effects, one must identify three levels of physical effects: (i) basic physical processes that directly determine the maser's observed output frequency; (ii) transducing factors that can affect the basic frequency-determining processes; and (iii) driving mechanisms that can vary the transducing factors. Fundamental frequency-determining processes include the cavity's resonance frequency, internal magnetic field, and collisional and wall frequency shifts. In addition, phase variations in the maser's amplifying and phase locking circuits can change the observed output frequency. Transducing factors include the cavity dimensions, the storage bulb's dielectric coefficient, the internal magnetic field strength and gradients, the beam flux, the atomic state distribution, and the properties of voltage dividers. Finally, intrinsic driving mechanisms – those independent of the environment – include the creep of material dimensions over time, long-term voltage reference aging, and aging of magnetic shield domains, while environmental driving mechanisms include temperature, humidity, barometric pressure, magnetic fields, and vibration. As an example of the three-step identification process, we note that both material dimension creep, an intrinsic mechanism, and temperature, an environmental mechanism, can affect the dimensions of the resonant cavity and, through the mechanism of cavity pulling, the maser's frequency.

Many of the three-step processes can be described analytically. The procedure is as follows:

1. Identify the frequency determining mechanisms, such as cavity pulling or internal magnetic field intensity.
2. Express the maser frequency f as a function of the relevant driving variables X_i , such as temperature, time, or external magnetic field.
3. Calculate the frequency variation δf as a differential:

$$\frac{\delta f}{f} = \sum \frac{1}{f} \frac{\partial f}{\partial X_i} \frac{\partial X_i}{\partial X_j} \delta X_j \quad (17)$$
4. Calculate or measure the sensitivities $\partial f / \partial X_i$ (e.g., $\partial f / \partial T_{\text{cavity}}$).
5. Estimate or measure the driving functions δX_j (e.g., δT_{cavity}).

As an example of this analytic approach, consider maser frequency variations due to changes in the cavity's resonance frequency that result from changes in the cavity's dimensions. Mechanisms that can affect the dimensions include bulk thermal expansion or contraction of the cavity's structural material, expansion or contraction of the cavity's metallic coating, relaxation of the coating's internal stress, and contraction of the cavity's joints with time. The driving mechanisms are time and cavity temperature. The maser frequency variation due to these mechanisms can be written as

$$\delta f_c = \left[\frac{\partial f_c}{\partial R} \frac{\partial R}{\partial T} + \frac{\partial f_c}{\partial L} \frac{\partial L}{\partial T} + \frac{\partial f_c}{\partial \sigma_s} \frac{\partial \sigma_s}{\partial T} \right] \delta T + \left[\frac{\partial f_c}{\partial \sigma_s} \frac{\partial \sigma_s}{\partial t} + \frac{\partial f_c}{\partial L} \frac{\partial L}{\partial t} \right] \delta t \quad (18)$$

Here R and L are the cavity's radius and length, σ_s is the coating's internal surface stress, T is the cavity's temperature, and t is elapsed time.

We consider those terms involving thermal expansion of the bulk cavity material. It can be shown that the fractional change in resonance frequency with temperature is given by

$$\frac{1}{f_c} \frac{df_c}{dT} = -\alpha \quad (19)$$

where α is the linear coefficient of expansion of the cavity material, assumed to be isotropic. Consequently, the maser frequency varies with temperature, due to bulk expansion, as

$$\frac{1}{f} \frac{\partial f_o(\text{bulk})}{\partial T} = -\alpha \left(\frac{Q_c}{Q_t} \right) = -\alpha \times 10^{-5} \quad (7)$$

for $(Q_c/Q_t) = 10^{-5}$, a typical value for SAO VLG-12 masers. The effect of bulk expansion on cavities made of different materials can readily be estimated. Table 1 gives the maser frequency variations expected to result from a cavity temperature variation of 10^{-5} °C for cavities made of low-expansion Cervit or Zerodur and of metals such as copper or aluminum.

Some processes that affect the maser's frequency are not amenable to calculation or measurement. An example are magnetic field effects. The maser frequency is affected by the average magnetic field intensity in the storage bulb through the quadratic hyperfine level dependence on magnetic field^[7] – the Breit-Rabi – shift, and also by magnetic field gradients through collisional (Crampton-Verhaar) shifts^[8]. While the field magnetic intensity, which drives the Breit-Rabi shift, can be measured, the internal field gradients, which affect the collisional shifts, are difficult or impossible to calculate or measure. However, the atomic state distribution in the beam, which also affects the collisional shifts, is both measurable and controllable, through single-state selection. If all atoms are in the "c" state, the collisional shifts are predicted to be zero. Fig. 5 shows measured sensitivities to external magnetic field variations with an AFP system both off and on. The solid lines represent the value of $\partial f/\partial B$ predicted by the Breit-Rabi equation from the measured change in field intensity. It is clear that use of single-state selection substantially eliminates the collisionally-induced field sensitivity.

Summary of Systematic Effects

An examination of a substantial number of systematic effects^[1] is summarized in Fig. 6. The calculations assume attainable values of environmental driving functions and maser sensitivities; for example, control of the maser cavity to 10^{-5} °C is assumed. Solid lines indicate ranges of variables that are fairly well understood, while dashed lines indicate ranges that could occur if special care is not taken. Dotted lines represent variables whose behavior is not well characterized. In particular, the long-term constancy of the wall shift is an area needing careful investigation.

It will be seen that most known effects are at the low 10^{-16} level. Thermal changes in storage bulb dielectric coefficient, possible cavity dimensional aging, and possible external magnetic field variations are predicted to predominate at that level. Improving the stability below 1 part in 10^{16} will clearly require attention to many effects simultaneously.

ACKNOWLEDGEMENT

This work was supported by the Jet Propulsion Laboratory.

References

1. The material in the present paper is discussed more extensively in work sponsored by the Jet Propulsion Laboratory and reported in: E.M. Mattison and R.F.C. Vessot, Final Report on JPL contract 958019, "A study on the feasibility of development of a state-of-the-art hydrogen maser," October, 1989.
2. Allan, D.W., "Statistics of atomic frequency standards," *Proc. I.E.E.E.* 54, 221-230 (1966).

3. D. Kleppner, H.C. Berg, S.B. Crampton, N.F. Ramsey, R.F.C. Vessot, H.E. Peters and J. Vanier, "Hydrogen maser principles and techniques," *Phys. Rev. A* **138**, 972 (1965).
4. R.F.C. Vessot, L. Mueller, and J. Vanier, "The specification of oscillator characteristics from measurements in the frequency domain." *Proc. I.E.E.E.* **54**, 199-207 (1966). See also W. A. Edson, "Noise in oscillators," *Proc. IRE* **48**, 1454-1456 (1960).
5. Berlinsky, A.J., and Hardy, W.N., in *Proc. of 13th Annl. Precise Time and Time Interval Meeting*, U.S. Naval Research Laboratory, December 1-3, 1981, pp. 542-562.
6. J. Vanier and C. Audoin, *The quantum physics of atomic frequency standards*, Adam Hilger, Philadelphia (1989).
7. N.F. Ramsey, "Molecular Beams," Clarendon Press (1956). P.86.
8. J.M.V.A. Koelmann, S.B. Crampton, H.T.R. Stoof, O.J. Luiten and B.J. Verhaar, "Spin exchange frequency shifts in cryogenic and room temperature hydrogen masers," *Phys. Rev. A*, **35**, 3825 (1987).

Cavity Material	α ($^{\circ}\text{C}^{-1}$)	$(1/f)(\partial f_0/\partial T)$ ($^{\circ}\text{C}^{-1}$)	$\delta f/f$ ($\delta T=10^{-5}$ $^{\circ}\text{C}$)
Cervit or Zerodur	-1×10^{-7}	1×10^{-12}	1×10^{-17}
Copper or Aluminum	$+2 \times 10^{-5}$	-2×10^{-10}	2×10^{-15}

Table 1. Frequency Variations Due to Cavity Bulk Expansivity

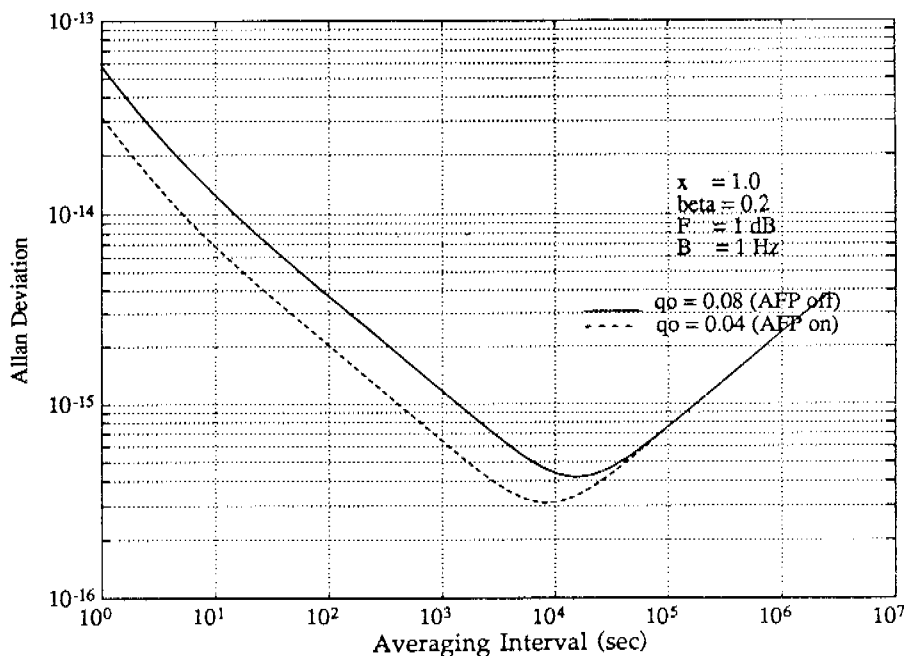


Fig. 1. Effect of State Selection on Frequency Stability

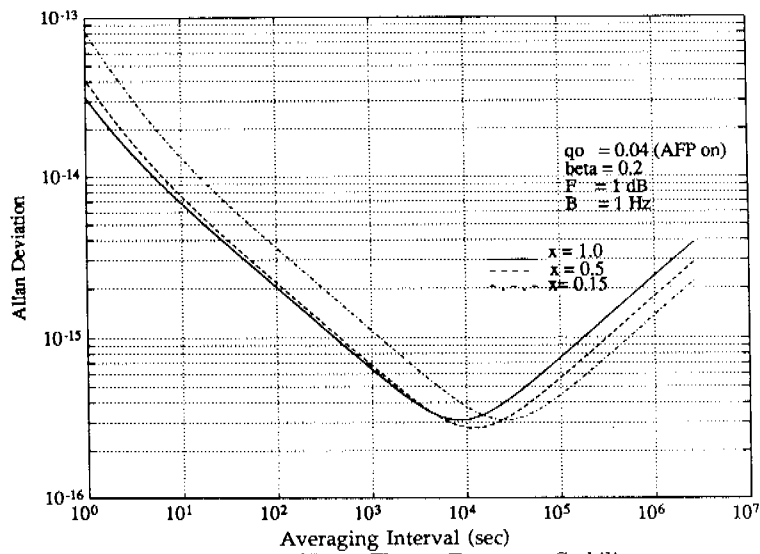


Fig. 2. Effect of Beam Flux on Frequency Stability

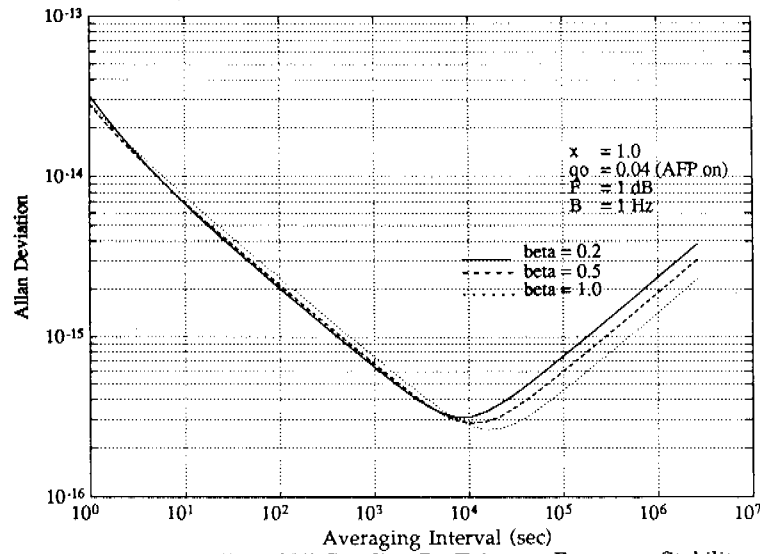


Fig. 3. Effect of RF Coupling Coefficient on Frequency Stability

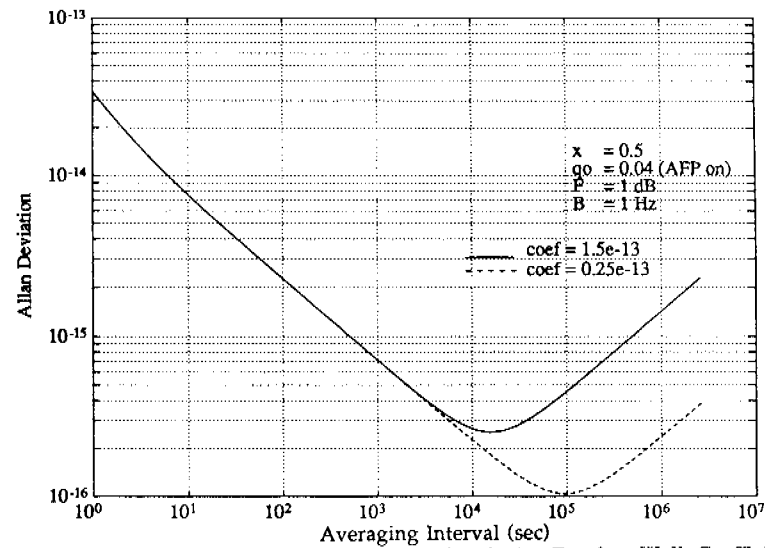


Fig. 4. Effect on Frequency Stability of Reducing Random-Walk Coefficient

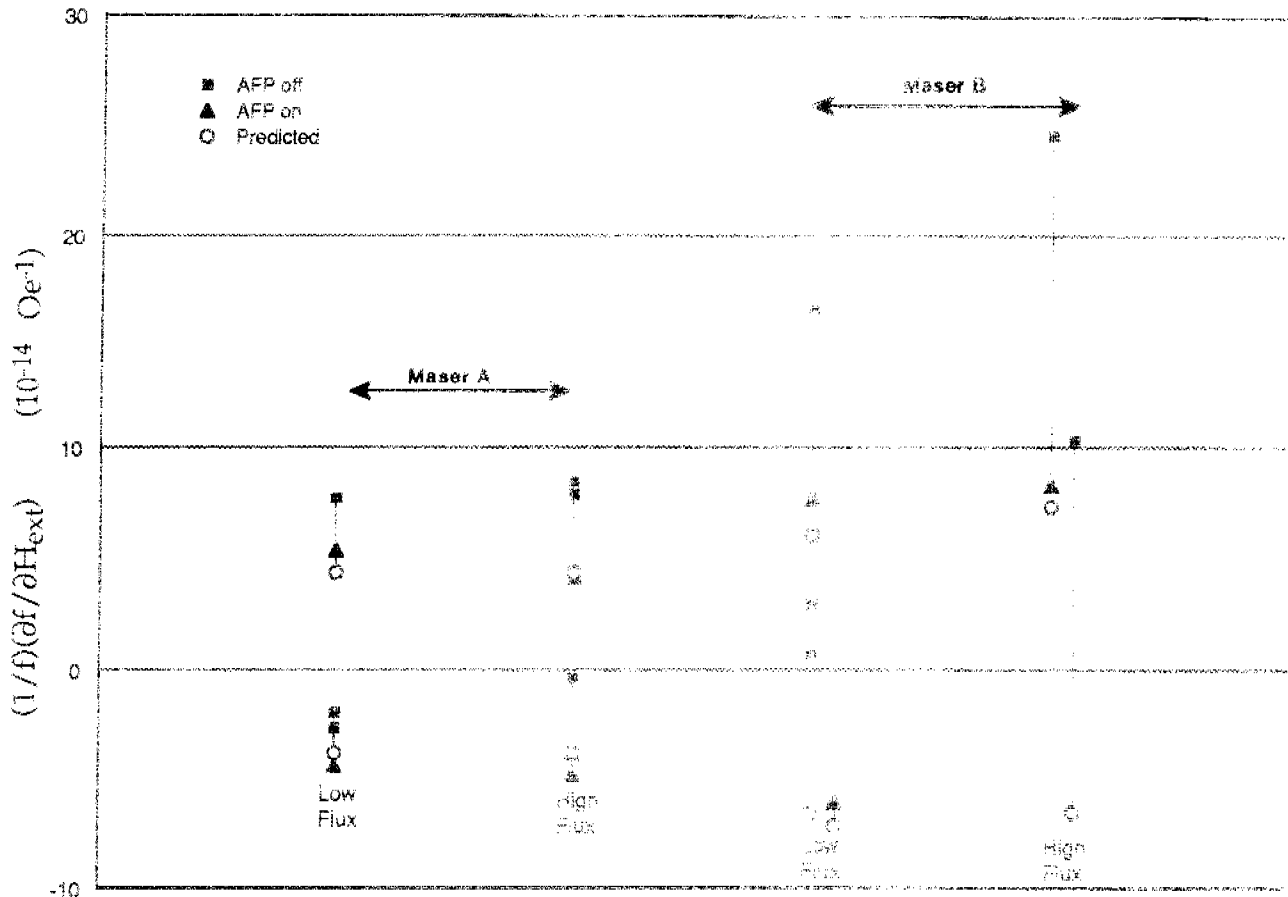


Fig. 5. Effect of State Selection on Magnetic Sensitivity

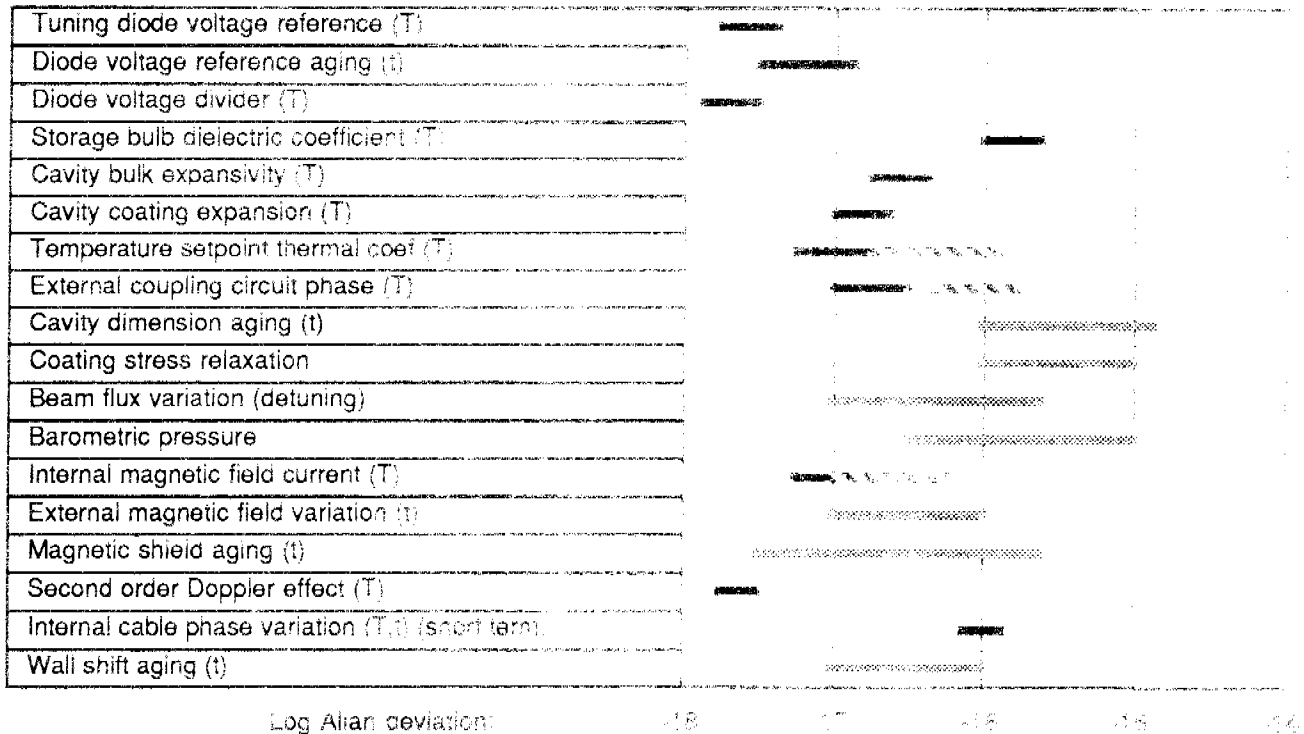


Fig. 6. Summary of Systematic Effects on Maser Frequency Stability

QUESTIONS AND ANSWERS

JACQUES VANIER, NRC: You have built several masers over the years. Different masers have different line Q's. Could you comment on the correlation between the line Q and the long term stability? Does it depend on the line Q or on all these other parameters.

MR. MATTISON: Until recently, most of our masers have had line Q's between 1 and 2 times ten to the ninth. It is only recently, with the VLG12 masers that we have had line Q's of 5 times ten to the ninth. We really don't have good measurements of the long term stability of them yet. They are now at USNO and that is where we are going to find out. I assume that Dr. Winkler will let us know about their long term stability.

TOM ENGLISH, BALL CORP.: I noticed on your last view graph that you had a mechanism called 'dielectric constant of the storage bulb'. Could you just say a few words about that?

MR. MATTISON: In the maser the storage bulb is made of quartz which acts to load the cavity. The dielectric constant of the quartz changes with temperature and therefor changes the resonant frequency of the cavity. That is quite a significant effect. **HARRY PETERS, SIGMA TAU:** I just wanted to say that some of the considerations of optimization relative to power output, cavity Q etc. do not necessarily apply to all configurations of hydrogen masers. If you have a cavity switching servo such as ours have, your signal-to-noise ratio for your servo system depends on your amplitude of oscillation and the power coupled out. Therefor, you tune more precisely with more power out and you might want to use a much higher Q cavity than if you were not tuning this way. There are a few other parameters which may differ if you are considering other automatic tuning systems.

MR. MATTISON: With any analytic approach such as this, the results depend on the model that you are using. Clearly, as you say, if tuning is another process involved, you have to include that in the calculation. It was not including here.